Geoscience and Remote Sensing (2022)
Clausius Scientific Press, Canada

DOI: 10.23977/geors.2022.050105
ISSN 2523-2592 Vol. 5 Num. 1

Remote Sensing Image Prediction of Water Environment Based on 3D CNN and ConvLSTM

Li Wang[1], Wenhao Li[1,*], Xiaoyi Wang [1,2], Jiping Xu[1], Zhiyao Zhao[1], Jiabin Yu[1], Huiyan Zhang[1], Qian Sun[1], Yuting Bai[1]

[1]Beijing Laboratory for Intelligent Environmental Protection, Beijing Technology & Business University, Beijing, China
[2]Beijing Institute of Fashion Technology, Beijing, China
[*]Corresponding author

Keywords: water eutrophication, remote sensing image, prediction, convolutional long and short time neural network

Abstract: The current research on cyanobacterial bloom prediction is mainly conducted by collecting data in the field and sending them to the laboratory for analysis to obtain water quality data, this method is affected by the weather and does not show the whole water information. Remote sensing images have been used more and more in water bloom prediction due to their high accuracy and convenient acquisition methods, but the accuracy of existing bloom prediction methods based on remote sensing image is low. To solve this issue, a water bloom prediction model based on convolutional long-short time network and 3DCNN network is proposed in this paper, which can predict the remote sensing images of future time by inputting the remote sensing images of historical time, and the eutrophication level of water body of future time can be obtained by analysing the remote sensing images of future time, and then realize the prediction of cyanobacterial water bloom outbreak. To validate the method proposed in this paper, two-dimensional convolutional neural network and three-dimensional convolutional neural network are used as comparative experiments. The experimental results show that the prediction accuracy of the cyanobacterial bloom prediction model proposed in this paper is significantly better than t other two neural network models, which proves the effectiveness of the method in this paper.

1. Introduction

With the accelerated industrialization of societies around the world, the problem of water pollution has been intensifying everywhere since the 21st century [1]. According to the China Ecological Environment Bulletin in 2022, the current water quality monitoring of surface water monitoring points in major rivers and lakes in China shows that the water quality sections of Class I, II, III, IV, V and inferior V account for 3.4%, 30.4%, 29.3%, 20.9%, 6.8% and 9.2% respectively. Therefore, regular monitoring of water quality is needed to prevent the occurrence of eutrophication and water wars in water bodies. The traditional way of water quality monitoring is by placing a

certain number of monitoring points in the waters, and then measuring and analyzing the resultant data by manual sampling at a later stage. Although this method has a certain effect, But this requires a lot of labor and money, and is easily affected by external factors such as weather, which is very easy to cause the instability of the results. At the same time, the location data of the station can only be used for part of the water. Therefore, there is a need to study the method to predict the spatial and temporal distribution of water eutrophication in the whole water area. Water quality monitoring through remote sensing images can achieve dynamic monitoring and early warning of water eutrophication. Remote sensing refers to the detection of ground objects by artificial satellites in the form of electromagnetic waves and collect information to determine the nature and state of the target. At present, remote sensing technology has been widely used in meteorological observation, ocean monitoring, environmental pollution monitoring, etc., which provides a lot of convenience and support for human activities.

Current prediction methods for cyanobacterial blooms are mainly divided into mechanism-driven and data-driven prediction methods.

Mechanistic models are accurate mathematical models with definite physical meaning based on the principles of the thing itself or the occurring process [2-5]. The mechanism-driven model can be adjusted to the model at any time according to different parameters and has stability. However, a large number of parameters need to be set, which can easily interfere with the results.

Data-driven models analyze the interrelationship between cyanobacterial bloom growth process and internal and external environmental factors by monitoring a large amount of historical data, and are further divided into two categories: mathematical statistical models and artificial intelligence models. Mathematical statistical models analyze the role of influencing factors on state variables by processing historical data of state variables and discovering the development pattern of variables by using regression analysis and correlation analysis[6-9]. Artificial intelligence models mainly contain traditional machine learning and deep learning methods. Traditional machine learning shows strong self-learning and self-adaptive capabilities when dealing with nonlinear problems such as cyanobacterial water bloom outbreaks, but the fitting ability is weak and can not learn large amounts of data[10-14]; deep learning is a type of representation learning [15] that automatically extracts high level abstract features from data without having to set features manually [16], and the model capability grows exponentially with depth[17]. The main deep learning networks commonly used in cyanobacterial bloom prediction are convolutional neural networks [18], recurrent neural networks[19], graph neural networks[20], and their improved and combined network models [21-22].

Therefore, the research of this thesis is to study the spatial and temporal distribution prediction method of water eutrophication for the whole water area based on remote sensing image data, using a method that is suitable for processing image data and can predict the trend of future moments of remote sensing image, and to effectively model and analyze the water eutrophication to achieve the spatial and temporal distribution prediction of water eutrophication for the whole water area. Specifically, this paper proposes to combine a one-layer 3D convolutional neural network(3D CNN) with a two-layer convolutional long and short time neural network(ConvLSTM). ConvLSTM is suitable for image sequence prediction of two-dimensional images, and the convolutional neural network can extract features directly from the input remote sensing images of water eutrophication, which reduces the manual involvement. The combination of the two can improve the spatial correlation between the predicted remote sensing images and the overall spatial correlation of water bodies.

2. Remote Sensing Image Prediction Method Based on Convlstm

To address the problem that existing image prediction methods are difficult to deal with the prediction of time series images, this paper proposes to combine a one-layer 3D CNNwith a two-layer ConvLSTM. First, the ConvLSTM is used to predict the remote sensing image at a future time, and then 3D CNN is used to adjust the image dimension to predict the remote sensing image at a future time.

2.1. Principle of Long and Short Term Memory Neural Network

Long Short-Term Memory (LSTM) is different from recurrent neural networks, which are only suitable for keeping short-term tasks, and has a greater advantage in the analysis of long sequence data, which can be recognized afterwards by the input from long time ago. Usually in human brain memory, people tend to remember more important things more clearly. According to this principle LSTM introduces the mechanism of gate, when the value of the gate is 0 it means that the information is discarded and when the value is 1 it means that the information is retained. The input gate determines which new information is remembered, while the forgetting gate determines which original information is retained, and the output gate determines the extent of the output information. LSTM combines and sums the sigmoid and tanh functions, which effectively reduces the gradient disappearance compared to RNNs with only the tanh function for activation. The structural schematic of the LSTM is shown in Figure 1.

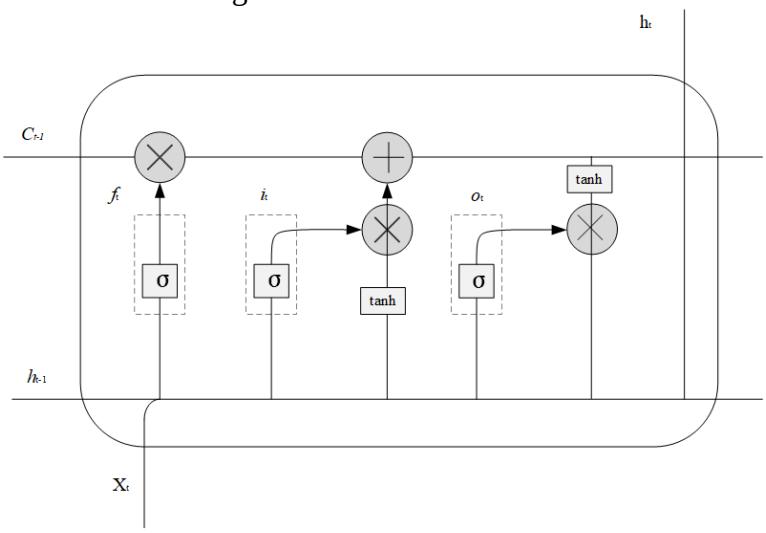

Figure 1: LSTM neural network

The input vector of a single LSTM memory block is x_t, and the forward propagation formula can be expressed as follows. Long-term memory unit C_t update process:

$$i_t = \partial(W_{xi}x_t + W_{hi}H_{t-1} + b_i) \tag{1}$$

$$f_t = \partial(W_{xf}X_t + W_{hf}H_{t-1} + b_f) \tag{2}$$

$$\tilde{C}_t = \tanh(W_{xc}X_t + W_{hc}H_{t-1} + b_c) \tag{3}$$

$$C_t = f_t C_{t-1} + i_t \tilde{C}_t \tag{4}$$

Here: f_t represents forgetting gate, i_t represents input gate, $W_{\sim i}$, $W_{\sim f}$, $W_{\sim c}$ are weight parameters, and long-term memory unit b_i, b_f, b_c are the bias terms of the input gate, forgetting gate, and long-term memory unit. The input gate controls the degree of writing the new memory $\tilde{C}_t$ into the long-term memory. f_t,i_t, $\tilde{C}_t$ are all functions related to the short-term memory H_{t-1} at the previous moment and the input X_t at the current moment. σ is a sigmoid function.

2.2. Principle of Convolutional Long and Short Time Neural Network

The ConvLSTM neural network is a combination of CNN and LSTM models. Convolutional LSTM (ConvLSTM) can be further optimized in terms of spatial correlation and better anti-interference in data than the traditional LSTM model, which can be used to extract local features by convolution while building time series models with long and short time to achieve good prediction results. The convolutional long-short time model is applied to various kinds of prediction problems based on spatio-temporal sequences. For the remote sensing images studied in this paper, the ConvLSTM network can be used to convolve the input remote sensing images by picture sequence to extract the waterwarp features and better achieve the prediction of time-series data pictures. The structure schematic of ConvLSTM network is shown in Figure 2.

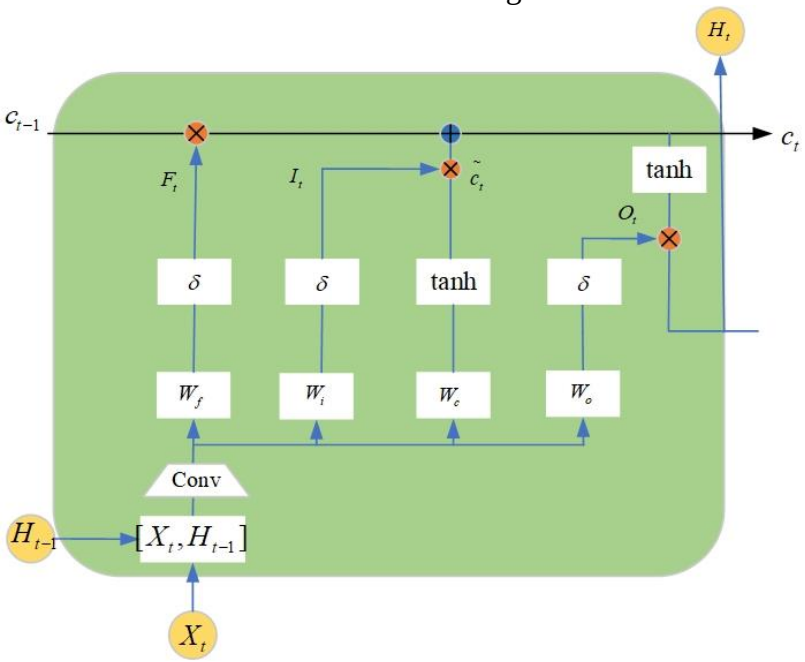

Figure 2: ConvLSTM structure diagram

As shown in Figure 2, ConvLSTM is comprised of 3 gate control units and 1 central node. The biggest difference from LSTM is that single-layer convolution calculation is performed after the current time input and short-term memory are combined. This difference is the key to extracting spatial structure information. ConvLSTM can be described as:

$$I_t = \sigma(W_{xi} * X_t + W_{hi} * H_{t-1} + b_i) \tag{5}$$

$$F_t = \sigma(W_{xf} * X_t + W_{hf} * H_{t-1} + b_f) \tag{6}$$

$$\tilde{c}_t = \tanh(W_{xc} * X_t + W_{hc} * H_{t-1} + b_c) \tag{7}$$

$$O_t = \sigma(W_{xo} * X_t + W_{ho} * H_{t-1} + b_o) \tag{8}$$

$$c_t = f_t \circ c_{t-1} + i_t \circ \tilde{c}_t \tag{9}$$

$$H_t = O_t \circ \tanh(c_t) \tag{10}$$

Here, * denotes convolution operation, ◦ denotes Hadamard product, σ denotes sigmoid function, $W_{x\sim}$ and $W_{h\sim}$ denotes 2-dimensional convolution kernel, X_t denotes input image at the current time, c_t denotes long-term memory, $\tilde{c}_t$ denotes newly generated information, H_t denotes short-term memory at the Current Moment, I_t denotes input gate output, F_t denotes forgetting gate output and O_t output gate output.

2.3. 3DCNN Principle

To extract inter-frame connectivity relationships between consecutive images, 3D-CNN adds a temporal dimension to traditional convolutional neural networks. By superimposing multiple feature maps in the form of video frames into a cube in which a 3D convolution kernel performs convolution operations in three dimensions: height, width, and depth, features in both temporal and spatial dimensions can be extracted. In 3DCNN, 3D convolution is first performed on the convolution layer to extract spatio-temporal information from the previous cube, after which a bias is added and the output is performed by an activation function. Since the feature extraction is performed using a 3D convolution kernel, multiple neighboring frames can be extracted simultaneously to obtain motion information. The feature map at the location of the first layer of the layer is calculated by taking the values as shown in Equation (11).

$$v_{ij}^{xyz} = f(b_{ij} + \sum_{m}\sum_{p=0}^{P_i-1}\sum_{q=0}^{Q_i-1}\sum_{r=0}^{R_i-1}\omega_{ijm}^{pqr} v_{(i-1)m}^{(x+p)(y+q)(z+r)}) \tag{11}$$

$f(\cdot)$ represents activation function, b_{ij} is bias of the j th feature map of the ith layer m is to traverse all points on the feature map at layer *i-1*, P_i is the height of the convolution kernel, Q_i is the width of the convolution kernel, R_i is the depth of the convolution kernel, ω_{ijm}^{pqr} is the value of the mth feature map at (p,q,r) connected to the *i-1*th layer, $v_{(i-1)m}^{(x+p)(y+q)(z+r)}$ is the value at (x+p,y+q,z+r) in the mth feature map of the *i-1*th layer. In the convolution process, the 3D convolution kernel performs convolution operation on continuous images with fixed step size, and various higher-order features are obtained by selecting different sizes of convolution kernels. At the same time, the downsampling operation also needs to be extended to the 3D level to summarize and integrate statistical features, reduce the data dimensionality and improve the operation efficiency.

2.4. Principle of Remote Sensing Image Prediction Based on ConvLSTM

By constructing a ConvLSTM network for remote sensing image prediction, the ConvLSTM network model contains two layers of convolutional long and short time neural network and one layer of 3D CNN network to realize the prediction for remote sensing images. The principle diagram of remote sensing image prediction based on ConvLSTM is shown in Figure 3.

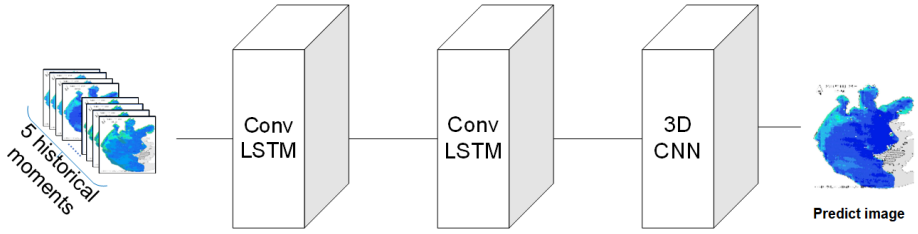

Figure 3: Schematic diagram of remote sensing image prediction based on ConvLSTM network

As shown in Figure 3, five images of historical moments are superimposed on the channel and fed into two layers of convolutional long-short time network for prediction, and finally the dimensionality is adjusted by a layer of 3Dcnn network to realize remote sensing images of future moments for prediction.

3. Water Eutrophication Prediction Methods and Applications Based on Remote Sensing Image

3.1. Flow of Water Eutrophication Prediction Based on Remote Sensing Images

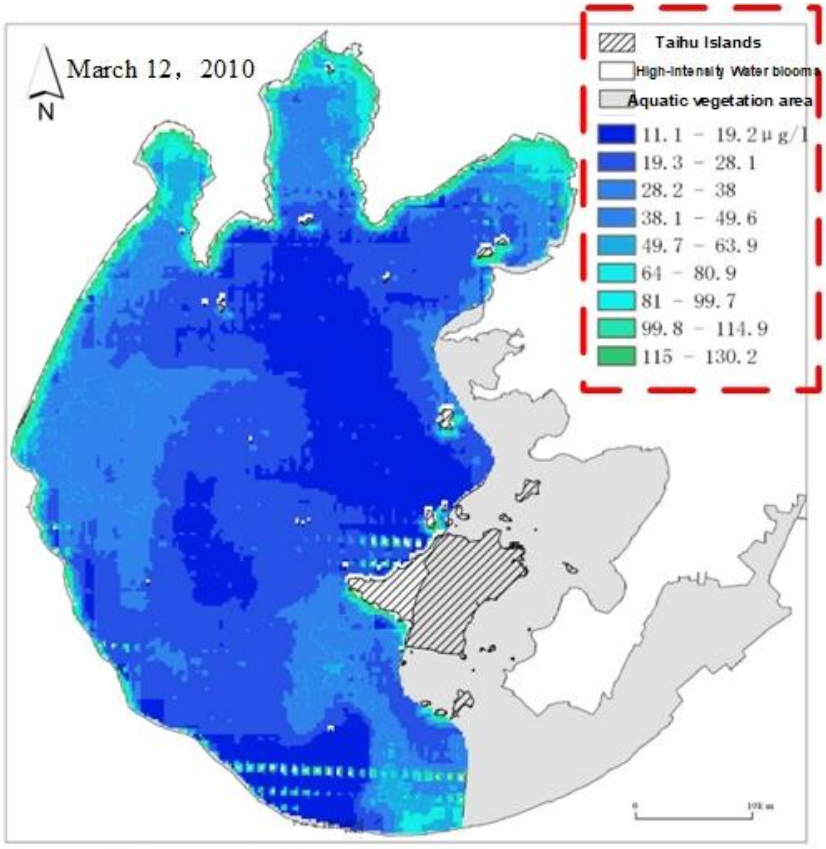

Figure 4: Remote sensing image of chlorophyll a concentration

The remote sensing image dataset in this paper is the inverse map of chlorophyll-*a* concentration from remote sensing image acquisition of water bodies in Taihu Lake region by MODIS satellite at the same moment of each day. In this paper, 169 sets of data from 2010-2011 were selected and sampled at the same moment every day starting from July 7, 2010 and ending on December 29, 2010. The first 148 sets for training and last 21 sets for testing. The image resolution was 256×256,

and the remote sensing images of chlorophyll-a concentration for every five days were input to predict the remote sensing images or the features of remote sensing images on the sixth day. Then, by pixel conversion of the predicted remote sensing images or a conversion model of the predicted remote sensing image features, average value of the predicted chlorophyll-a concentration is obtained, and the future level of water eutrophication occurrence is judged according to the eutrophication level of the water body, thus realizing the water eutrophication prediction. The inverse image of remote sensing image of chlorophyll-a concentration is shown in Figure 4.

The chlorophyll-a inversion diagram is a remote sensing image describing the relationship model between remote sensing data and chlorophyll-a concentration. The chlorophyll a concentrations in the graph are indicated using different colors, and the right side shows the labeled interval values of chlorophyll-a concentrations corresponding to different colors.

3.2. Flow of Water Eutrophication Prediction Based on Convlstm Remote Sensing Image Prediction

Figure 5 illustrates the overall flow chart of water body eutrophication prediction based on ConvLSTM remote sensing image prediction.

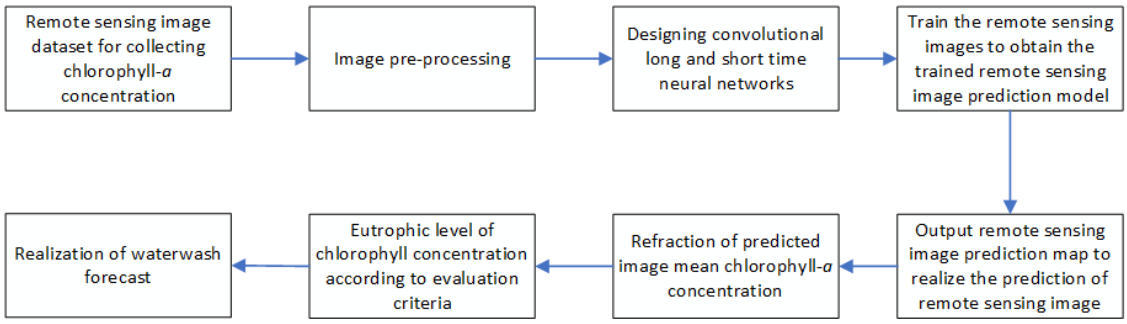

Figure 5: Flow chart of water eutrophication prediction based on ConvLSTM remote sensing image prediction

The ConvLSTM remote sensing image prediction process based on moisture prediction can be divided into the following points: Step 1, collect the remote sensing image dataset of Taihu Lake, sort the dataset according to the date, and divide the dataset and test set; Step 2, image pre-processing, compress the image pixels into 256x256 for input; Step 3, design the remote sensing image prediction model consisting of two layers of convolutional long-short time network and one layer of 3D convolutional neural network ;Step 4, Input training set and test set, adjust model parameters by training set and test model performance using test set; step 5, output the remote sensing image prediction map and comparison map to realize the prediction of remote sensing image; step 6, pixel conversion of the predicted remote sensing image to obtain the chlorophyll-a concentration of each pixel; step 7, determine the chlorophyll-a concentration of each pixel according to the evaluation criteria corresponding to the rich step 7, determine the chlorophyll-a concentration of each pixel corresponds to the nutrient rich level according to the evaluation criteria; step 8, realize the prediction of water eutrophication in each pixel position of the whole lake.

3.3. Results of Remote Sensing Image Prediction Based on ConvLSTM

The Convlstm prediction model constructed for this problem consists of two layers of ConvLSTM for prediction and one layer of 3D CNN for adjusting the dimensionality, and Table 1 shows the specific parameters of these three networks, and the model is iterated 200 times overall.

Table 1: Table of parameters of ConvLSTM model

Network layer	Number of convolution kernels	kernel size	Step	Padding method
ConvLSTM-1	64	2× 2	1 ×1	same
ConvLSTM-2	128	2× 2	1 ×1	same
3DCNN	3	1× 1 × 1	1 ×1 ×1	valid

The parameters in Table 1 are determined by the enumeration method as well as by the empirical method.The following is the remote sensing image prediction implemented based on the dataset and method introduced in the above paper. The excerpted original images of different dates are compared with the predicted images as shown in Figure 6.

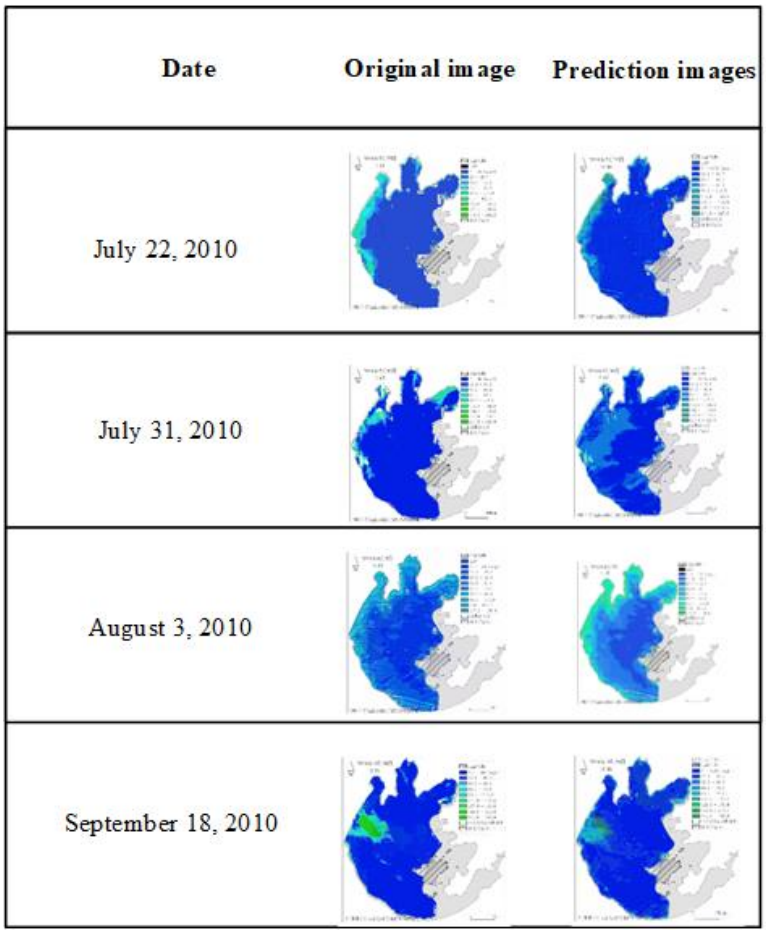

Figure 6: Comparison of original image and predicted image by ConvLSTM mode

Table 2: The values of each similarity evaluation

Model Name	Cosin	PSNR	SSIM	Mutual Information
ConvLSTM	0.997	21.624	0.842	1.352

In order to qualitatively evaluate the prediction results, we use several similarity indexes to evaluate the relationship between the predicted image and the real image, Table 2 shows the specific values of each similarity.

The higher the similarity between the predicted image and the original image, the closer the value of cosine similarity is to 1. The PSNR, which can be defined by the mean square error, the

larger the value, the less distortion represents the remote sensing image. The structural similarity takes the value range [0,1], and in this interval when the value is larger, it means the remote sensing image has less distortion. Mutual information is a description of the information relevance of one random variable to another, which can reflect the degree of dependence between them. The larger the mutual information in the neural network, the more similar the data set prediction is to the true distribution. From the similarity index, it can be seen that the prediction model proposed in this paper can well predict the remote sensing image in the future moment, and the predicted image is clearly and highly similar to the real image.

3.4. Conversion of Chlorophyll-A Concentration from Remote Sensing Images and Evaluation of Eutrophication Level of Water Bodies

The prediction for remotely sensed images is achieved by ConvLSTM model, and to achieve the prediction of water eutrophication also needs to determine the degree of eutrophication of chlorophyll-a concentration, so the predicted remotely sensed images need to be converted to chlorophyll-a concentration. The following is the conversion method of chlorophyll-a concentration.

By identifying the area of the pixel points corresponding to different colors, i.e., different chlorophyll-a concentrations, and then converting them. Taking Figure 4, i.e., the inversion map of chlorophyll-a on July 25, 2011, as an example, Table 3 shows the conversion process.

Table 3: Conversion table of chlorophyll-a concentration

Chlorophyll-a concentration (μg/L)	Mean chlorophyll- a concentration (μg/L)	Pixel dot area(px)	Mean area product
10-12.5	11.25	333398	3750727.5
12.6-18.6	15.6	0	0
18.7-30.2	24.45	33993	831128.85
30.3-44.3	35.3	0	0
44.4-61.3	52.85	16580	876253
61.4-81.2	71.3	0	0
81.3-102.6	91.95	10821	994990.95
102.7-153.7	128.2	0	0
153.8-244.9	199.35	4098	816936.3

As in the table above, the chlorophyll-a concentration pixel scale is first averaged, and the chlorophyll-a concentration range grade is averaged to identify the area of different bars of pixel points, respectively, and the area is 0 representing that the picture does not have this color i.e. this value contamination degree of water eutrophication.

$$c = \sum c_c s_c / s_a \tag{12}$$

c is the average chlorophyll-*a* concentration, $c_c$is the average chlorophyll-*a* concentration, and s_c is the corresponding pixel dot area, and the sum of the two products divided by the total area is the final chlorophyll-*a* concentration. For example, the sum of pixel dot area in the above table is 398890, and the product of the mean area is 7270036.6, and the average chlorophyll-*a* concentration is 18.23 μg/L obtained by dividing the latter by the former.

The eutrophication level of waters refers to the eutrophication grading standard of waters specified by the International Organization for Economic Cooperation and Development (OECD), and the nutrient level of lakes is poorly, moderately, eutrophically, and heavily eutrophic in four states.The specific values of the OECD eutrophication grading standard of water bodies are shown in Table 4.

Table 4: Water eutrophication classification standard (OECD)

Nutritional grade	Poor Nutrition	Medium Nutrition	Eutrophication	Heavy Eutrophication
Whole-lake chlorophyll-a Concentration(μg/L)	0~3.0	3.1~11.0	11.1~78.0	>78.1

In Table 4, nutritional grades of the lakes are divided into poor nutrition (< 3μg/L), medium nutrition (3.1~11μg/L), eutrophication (11.1-78.0μg/L), heavy eutrophication (> 78.1μg/L). However Taihu Lake is eutrophic throughout the year, and the fluctuations in chlorophyll-a concentrations cannot cover the entire classification range. Therefore, some scholars further subdivided the eutrophic grade in Table 1 into 4 grades Eutrophic I, II, III, and IV according to the actual situation, as shown in Table 5.

Table 5: Water eutrophication classification standard (Taihu Lake)

Nutritional grade	Poor nutrition	Medium Nutritional	Eutrophicatio-1	Eutrophicatio-2	Eutrophication-3	Eutrophicatio-4	Heavy Eutrophication
Whole-lake chlorophyll-a Concentration(μg/L)	0~3.0	3.1~11.0	11.1~20.0	20.1~22.0	22.1~24.0	24.1~78.0	>78.

According to the eutrophication grading criteria for Taihu Lake in the above table, Figure 4 with an average chlorophyll-a concentration of 18.23 μg/L can be classified as Eutrophicatio-1 as the prediction result of water eutrophication, and after the conversion of chlorophyll-a concentration and the judgment of eutrophic grade, the predicted remote sensing image results are transformed into the final prediction result of water eutrophication.

3.5. Prediction Results and Comparative Analysis of The Water Eutrophication

A comparison of the true values of chlorophyll-a concentration with the predicted values based on ConvLSTM is shown in Figure 7.

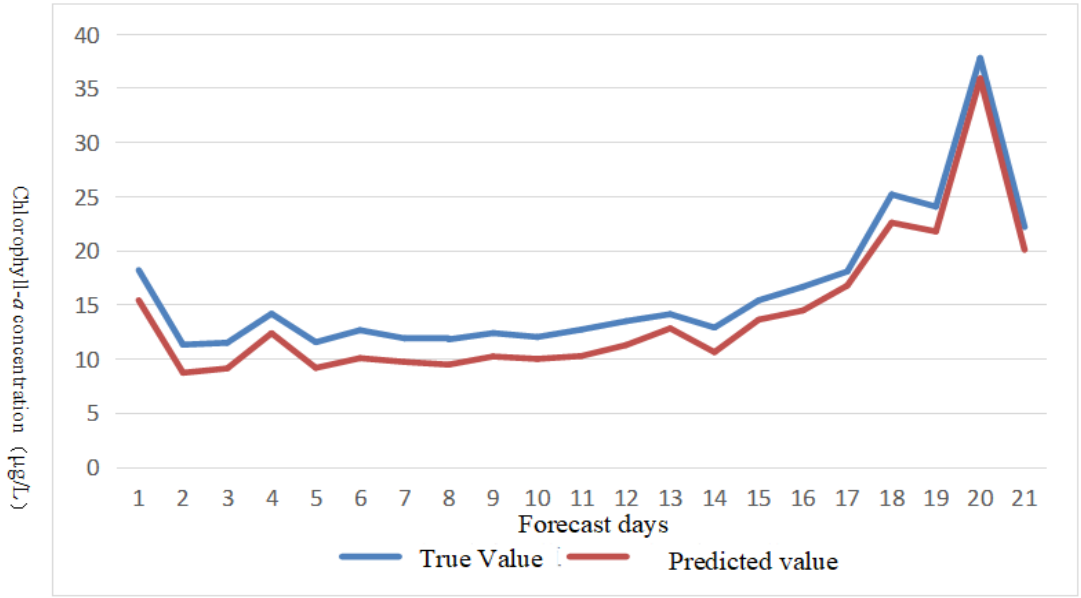

Figure 7: Comparison of true and predicted chlorophyll-a concentration based on ConvLSTM

The above figure compares the chlorophyll-a concentration of the 21-day predicted image with the original image, which reflects the prediction effect of the remote sensing prediction image based on ConvLSTM. In this experiment, the prediction results of chlorophyll-a concentration based on 2D-CNN and 3D-CNN remote sensing image feature extraction were taken as a comparison experiment, and in order to compare the prediction effects of the three methods on chlorophyll-a concentration, the standard error index was taken as a measure of the accuracy of the prediction results. The calculation is given in the following equation.

$$\mu = 1 - \left[\left(c_p - c_t \right)^2 / c_p \right] \tag{13}$$

Where μ is the accuracy, c_p is the predicted mean chlorophyll-*a* concentration, and c_t is the true value, and the accuracy results are shown in Table 6.

Table 6: The accuracy of chlorophyll-a concentration prediction by different models for the Lake Tai dataset

Model Name	Accuracy
2D-CNN	0.8804
3D-CNN	0.9397
ConvLSTM	0.9799

The above table shows that the ConvLSTM model has the highest accuracy. 3D-CNN has higher accuracy than 2D-CNN because 3D-CNN can consider both temporal and spatial influences to extract waterwarp features, while 2D-CNN has no temporal dimension, and at the same time 3D-CNN is more suitable for dynamic data processing. the ConvLSTM model combines 3D-CNN model with LSTM model Combining the advantages of 3D-CNN combines the features of extracting time series of LSTM model with the advantages of 3D-CNN, which is further optimized in spatial correlation and improves the anti-interference, so the accuracy is the highest. In summary, compared with 2D-CNN and 3D-CNN models, the predictive power of the ConvLSTM model is superior to the other two prediction models.

4. Conclusion

In this paper, by combining two layers of convolutional long-short time neural network and one layer of 3d convolutional neural network to form a convolutional long-short time model, we realize the prediction of remote sensing images and the prediction of water eutrophication by calculating the chlorophyll-a concentration . The main research work of this paper includes: (1) pre-processing remote sensing images and establishing a water eutrophication prediction model based on convolutional long and short time; (2) predicting future remote sensing images of water eutrophication by convolutional long and short time water eutrophication prediction model; (3) determining eutrophic level based on remote sensing images and calculating chlorophyll-a concentration of the whole lake to achieve prediction of water eutrophication; (4) calculate the evaluation indexes of the similarity between the predicted remote sensing image and the original image; (5) By comparing the eutrophication prediction method based on 2Dcnn and the eutrophication prediction method based on 3DCNN, it is confirmed that the prediction method based on ConvLSTM is better than the above two methods in terms of prediction accuracy, which shows the effectiveness of this model..

The innovation of this paper is to combine the convolutional long-short time neural network with remote sensing images, and the convolutional long-short time network has higher accuracy than 2D-CNN and 3D-CNN in prediction results The innovation of this paper is the combination of ConvLSTM network and 3D CNN network for eutrophication evaluation of water bodies. Since the

convolutional neural network can realize the processing of images, and the long-short time neural network can make prediction for time series, ConvLSTM is better than the traditional 2D convolutional neural network and 3D convolutional neural network in the temporal prediction of images.

Acknowledgement

Thanks to the National Social Science Fund of China No. 19BGL184 and the Beijing Excellent Talent Training Support Project for Young Top-notch Team No. 2018000026833TD01.

References

[1] Zhang JJ, Zhong CH, Deng CG. (2006) Discussion on definition of algal bloom. WATER RESOURCES PROTECTION, 22, 05, 45-47.
[2] W. M. Woelmer, R. Q. Thomas, M. E. Lofton, R. P. McClure, H. L. Wander, 2022, Near-term phytoplankton forecasts reveal the effects of model time step and forecast horizon on predictability. Ecological Applications, 1002, 2642.
[3] C. Y. Wang, Y. U. Yang, Y. K. Sun, L. H. Li, F. X. Kong et al. (2013) The discussion of the early forecasting of cyanobacteria bloom in the lake taihu based on elcom-caedym model. China Environmental Science, 33, 2, 491–502.
[4] X. Y. Wang, J. Jia, T. L. Su, Z. Y. Zhao, J. P. Xu et al. (2018) A fusion water quality soft-sensing method based on wasp model and its application in water eutrophication evaluation. Journal of Chemistry, 2018, 2018.
[5] X. M. Fan, L. X. Song, D. B. Ji, J. K. Shen, and D. F. Liu. (2017) Research on mechanism of algal blooms based on the critical depth theory. Environmental Science Technology, 40, 11, 89–94.
[6] Dillon P J, Rigler F. (1974) The phosphorus-chlorophyll relationship in lakes 1, 2. Limnology and oceanography, 19, 5, 767-773.
[7] Wang L, Gao C, Wang XY, et al. (2017) Nonlinear dynamics analysis and water bloom prediction of cyanobacteria growth time variation system. CIESC Journal, 68, 3, 1065-1072.
[8] Yan Q, Ma C. (2016) Application of integrated ARIMA and RBF network for groundwater level forecasting. Environmental Earth Sciences, 75, 5, 1-13.
[9] Wang L, Liu ZW, Wu CR, et al (2013) Water bloom prediction and factor analysis based on multidimensional time series analysis. SIESC Journal, 64, 12, 4649-4655
[10] Wu J, Zhu YL, Jin S, et al. (2020) Area prediction of cyanobacterial blooms based on three machine learning methods in Taihu Lake. Journal of Hohai University (Natural Sciences), 48, 6, 542-551.
[11] Liu YX, Wu H. (2018) Water Bloom Early Warning Model Based on Random Fores. YELLOW RIVER, 40,8, 75-77+90.
[12] Wang S, Wang ZH, Feng SL, et al. (2018) The Application of BP Neural Network in Forecasting Algal Blooms of Shanxi Reservoir. SICHUAN ENVIRONMENT, 37, 1, 39-43.
[13] Qi GH, Ma XS, He SY, et al. (2021) Long-term spatiotemporal variation analysis and probability prediction of algal blooms in Lake Chaohu (2009—2018) based on multi-source remote sensing data. Journal of Lake Sciences, 2021, 33, 2, 414-427.
[14] Wang ZF. (2017) Risk assrssment model for algal bloom of open channel based on dynamic Naïve Bayes classifier. South-to-North Water Transfers and Water Science &Technology, 15, 2, 89-94.
[15] Bengio Y, Courville A, Vincent P. (2013) Representation learning: A review and new perspectives. IEEE transactions on pattern analysis and machine intelligence, 35, 8, 1798-1828.
[16] Lecun Y, Bengio Y, Hinton G. (2015) Deep learning. nature, 521, 7553, 436-444.
[17] Delalleau O, Bengio Y. (2011) Shallow vs. deep sum-product networks. Advances in neural information processing systems, 33, 24.
[18] Wang J, Gao ZX, Zhu YM. (2021) Research on Yellow River Water Quality Prediction Based on CNN-LSTM Mode. YELLOW RIVER, 43(05):96-99+109.
[19] Li Y, Zhu Z, Kong D, et al. (2019) EA-LSTM: Evolutionary attention-based LSTM for time series prediction. Knowledge-Based Systems, 181, 104785.
[20] XU JH, Wang JC, Chen L, et al. (2021) Surface water quality prediction model based on graph neural network. Journal of Zhejiang University (Engineering Science), 55, 4, 601-607.
[21] YU JB, Shang FF, Wang XY, et al. (2018) Cyanobacterial bloom forecast method based on genetic algorithm-first order lag filter and long short-term memory network. Journal of Computer Applications, 38, 7, 2119-2123.
[22] Hwang S, Jeon G, Jeong J, et al. (2019) A novel time series based Seq2Seq model for temperature prediction in firing furnace process. Procedia Computer Science, 155, 19-26.